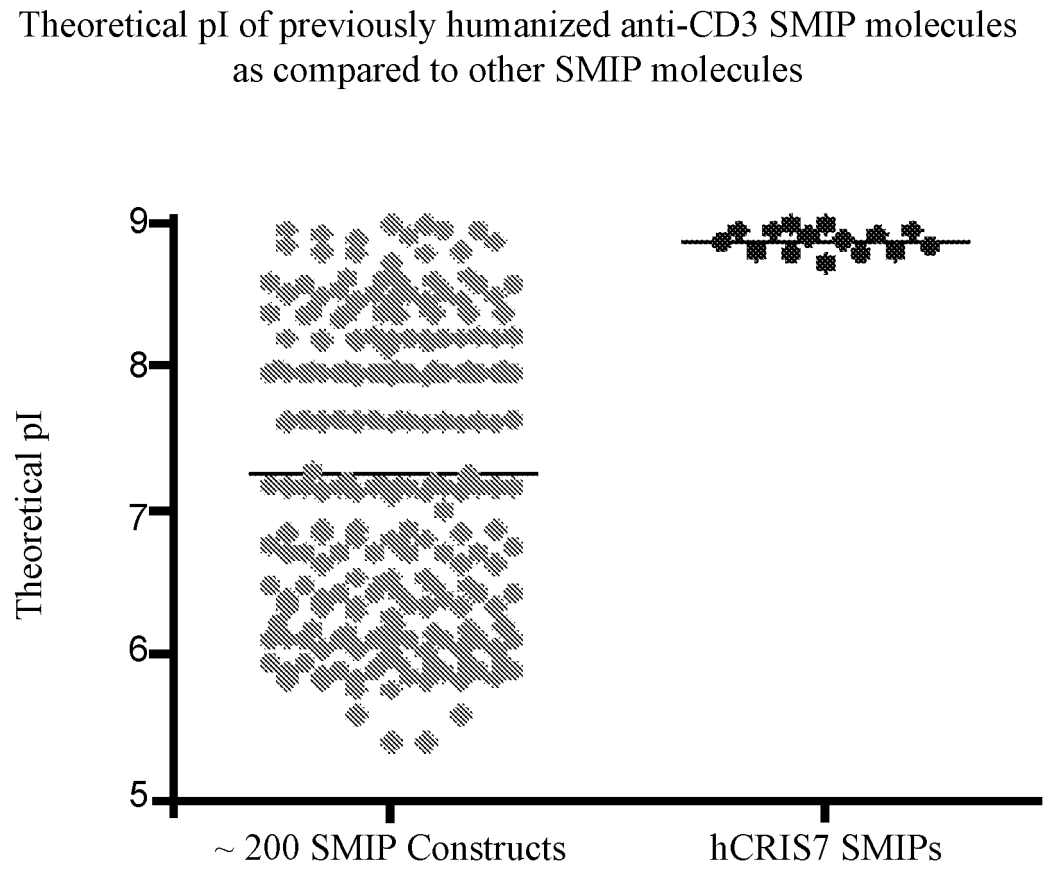
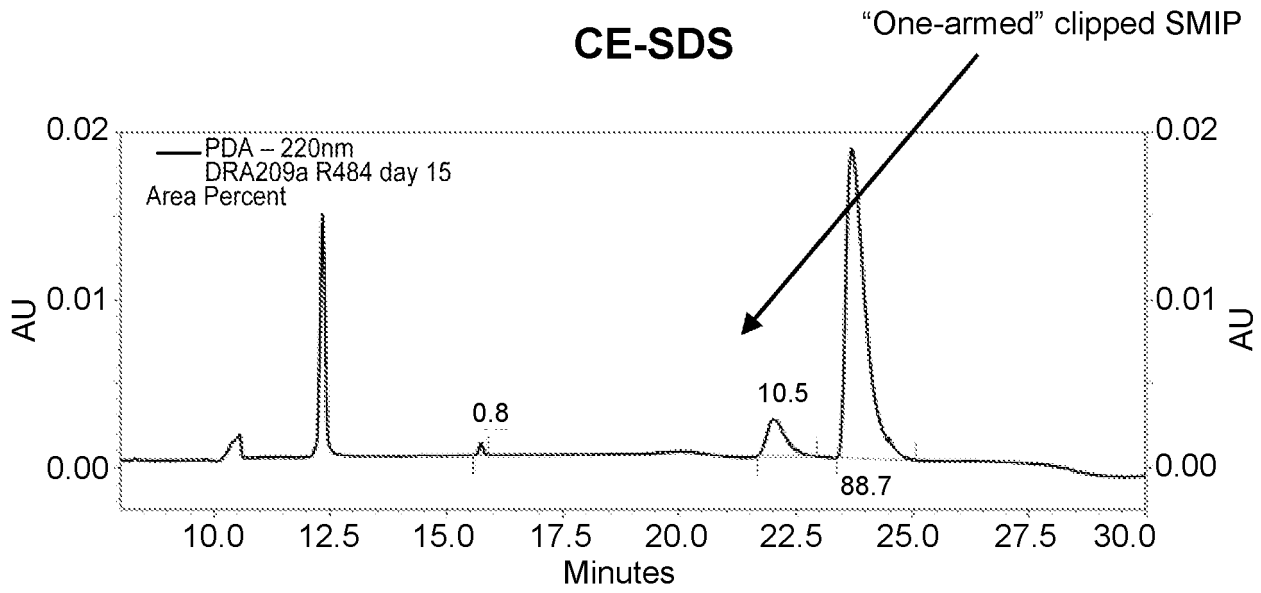

Theoretical pI of previously humanized anti-CD3 SMIP molecules as compared to other SMIP molecules
Theoretical pI
9
8
7
6
5
~ 200 SMIP Constructs
hCRIS7 SMIPs

FIG. 1



Clone 9D8, R484 (Reactor)

FIG. 2A

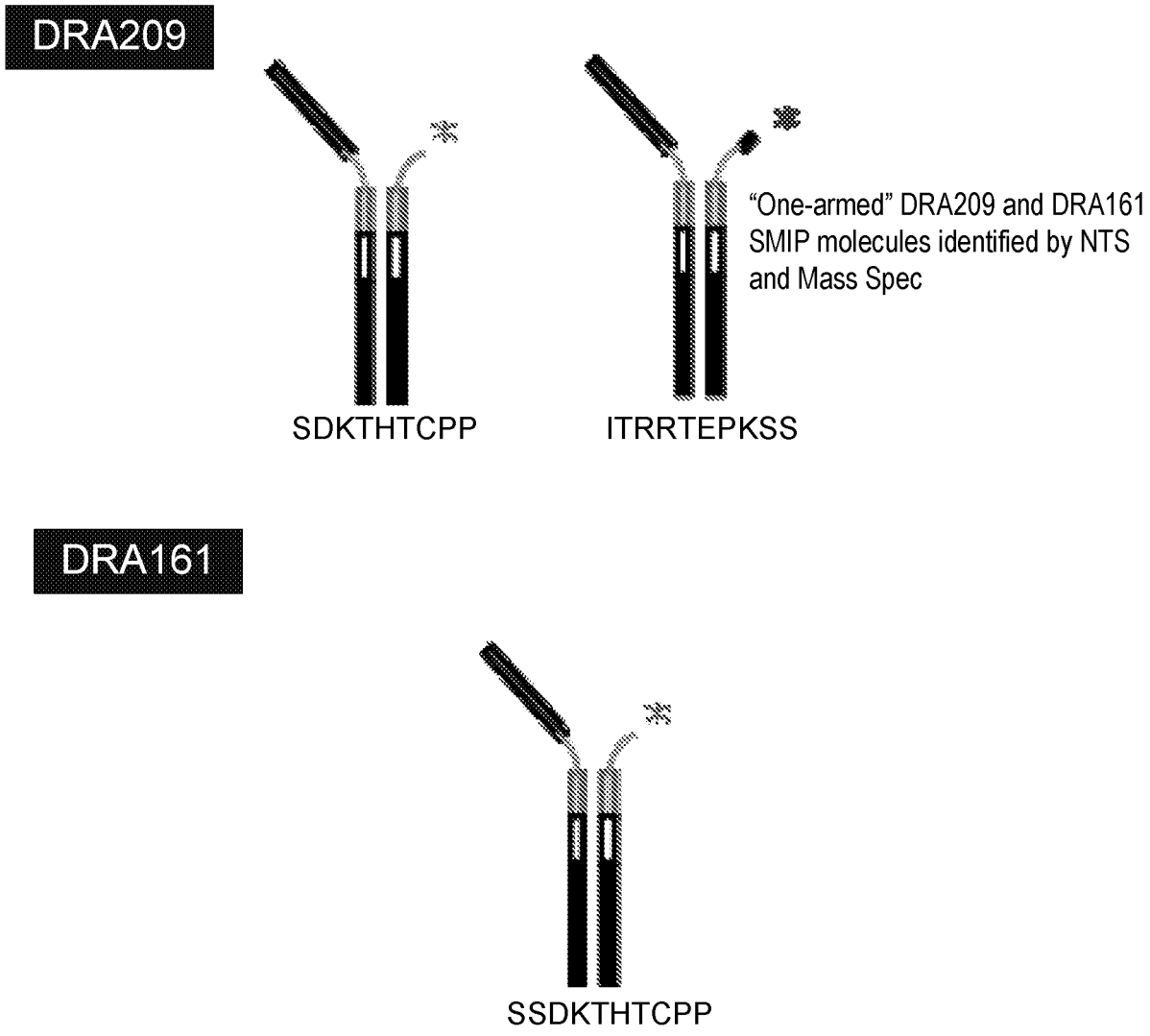

DRA209
SDKTHTCPP
ITRRTEPKSS
"One-armed" DRA209 and DRA161 SMIP molecules identified by NTS and Mass Spec
DRA161
SSDKTHTCPP

FIG. 2B

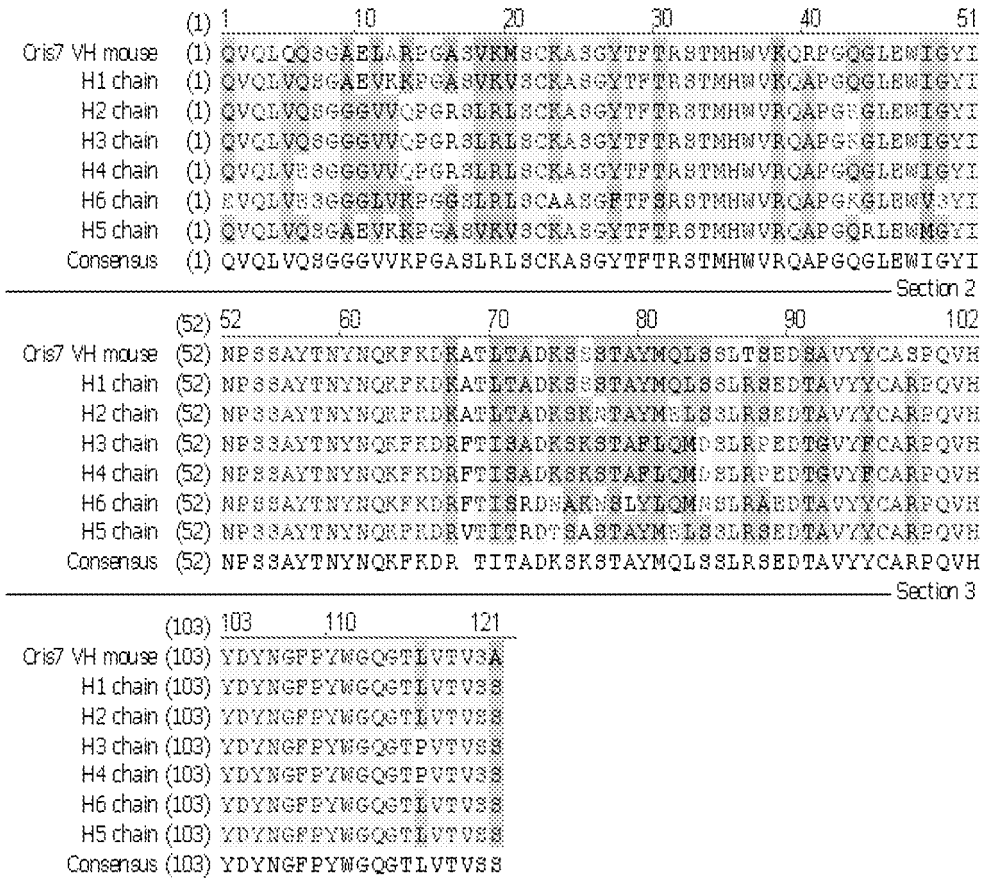

(1) 1 10 20 30 40 51
Cris7 VH mouse (1) QVQLQQSGAELARPGASVKMSCKASGYTFTRSTMHWVKQRPGQGLEWIGYI
H1 chain (1) QVQLVQSGAEVKKPGASVKVSCKASGYTFTRSTMHWVKQAPGQGLEWIGYI
H2 chain (1) QVQLVQSGGGVVQPGRSLRLSCKASGYTFTRSTMHWVRQAPGQGLEWIGYI
H3 chain (1) QVQLVQSGGGVVQPGRSLRLSCKASGYTFTRSTMHWVRQAPGQGLEWIGYI
H4 chain (1) QVQLVESGGGVVQPGRSLRLSCKASGYTFTRSTMHWVRQAPGQGLEWIGYI
H6 chain (1) EVQLVESGGGLVKPGGSLRLSCAASGFTFSRSTMHWVRQAPGKGLEWVSYI
H5 chain (1) QVQLVQSGAEVKKPGASVKVSCKASGYTFTRSTMHWVRQAPGQRLEWMGYI
Consensus (1) QVQLVQSGGGVVKPGASLRLSCKASGYTFTRSTMHWVRQAPGQGLEWIGYI
Section 2
(52) 52 60 70 80 90 102
Cris7 VH mouse (52) NPSSAYTNYNQKFKDKATLTADKSSSTAYMQLSSLTSEDSAVYYCASPQVH
H1 chain (52) NPSSAYTNYNQKFKDKATLTADKSSSTAYMQLSSLRSEDTAVYYCARPQVH
H2 chain (52) NPSSAYTNYNQKFKDKATLTADKSKNTAYMELSSLRSEDTAVYYCARPQVH
H3 chain (52) NPSSAYTNYNQKFKDRFTISADKSKSTAFLQMDSLRPEDTGVYFCARPQVH
H4 chain (52) NPSSAYTNYNQKFKDRFTISADKSKSTAFLQMDSLRPEDTGVYFCARPQVH
H6 chain (52) NPSSAYTNYNQKFKDRFTISRDNAKNSLYLQMNSLRAEDTAVYYCARPQVH
H5 chain (52) NPSSAYTNYNQKFKDRVTITRDTSASTAYMELSSLRSEDTAVYYCARPQVH
Consensus (52) NPSSAYTNYNQKFKDR TITADKSKSTAYMQLSSLRSEDTAVYYCARPQVH
Section 3
(103) 103 110 121
Cris7 VH mouse (103) YDYNGFPYWGQGTLVTVSA
H1 chain (103) YDYNGFPYWGQGTLVTVSS
H2 chain (103) YDYNGFPYWGQGTLVTVSS
H3 chain (103) YDYNGFPYWGQGTPVTVSS
H4 chain (103) YDYNGFPYWGQGTPVTVSS
H6 chain (103) YDYNGFPYWGQGTLVTVSS
H5 chain (103) YDYNGFPYWGQGTLVTVSS
Consensus (103) YDYNGFPYWGQGTLVTVSS

FIG. 3

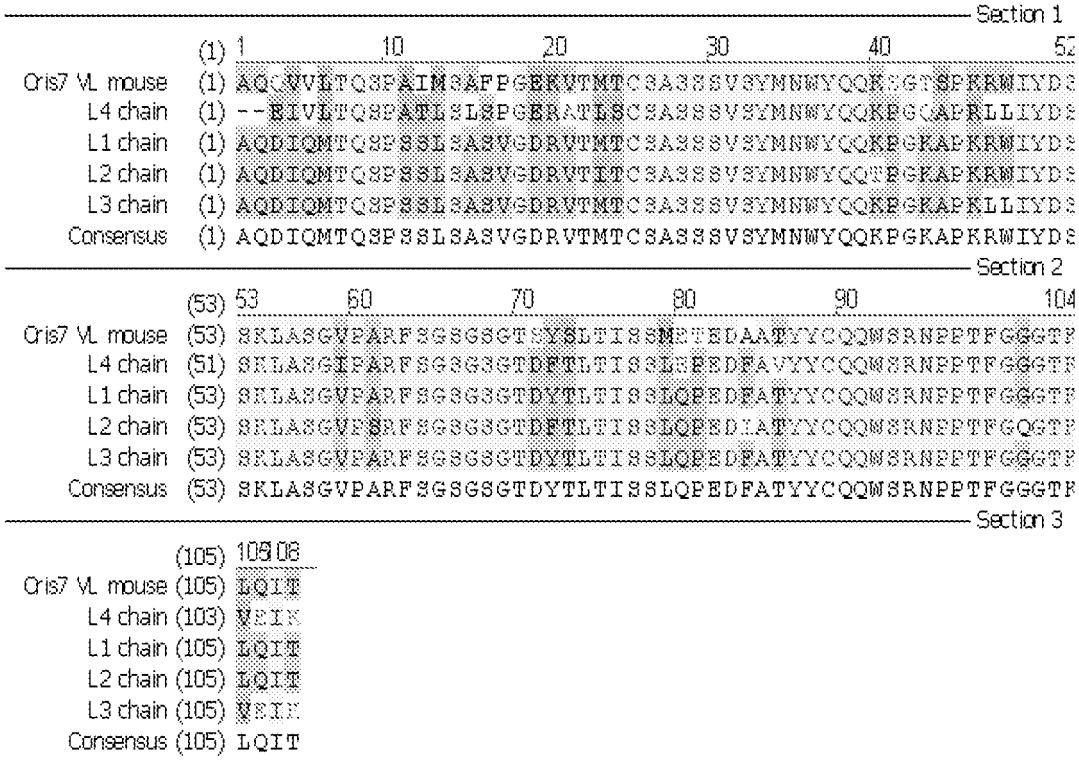

Section 1
Cris7 VL mouse (1) AQDVVLTQSPAIMSAFPGEKVTMTCSASSSVSYMNWYQQKSGTSPKRWIYDS
L4 chain (1) --EIVLTQSPATLSLSPGERATLSCSASSSVSYMNWYQQKPGQAPRLLIYDS
L1 chain (1) AQDIQMTQSPSSLSASVGDRVTMTCSASSSVSYMNWYQQKPGKAPKRWIYDS
L2 chain (1) AQDIQMTQSPSSLSASVGDRVTITCSASSSVSYMNWYQQTPGKAPKRWIYDS
L3 chain (1) AQDIQMTQSPSSLSASVGDRVTMTCSASSSVSYMNWYQQKPGKAPKLLIYDS
Consensus (1) AQDIQMTQSPSSLSASVGDRVTMTCSASSSVSYMNWYQQKPGKAPKRWIYDS
Section 2
Cris7 VL mouse (53) SKLASGVPARFSGSGSGTSYSLTISSMETEDAATYYCQQWSRNPPTFGGGTK
L4 chain (51) SKLASGIPARFSGSGSGTDFTLTISSLEPEDFAVYYCQQWSRNPPTFGGGTK
L1 chain (53) SKLASGVPARFSGSGSGTDYTLTISSLQPEDFATYYCQQWSRNPPTFGGGTK
L2 chain (53) SKLASGVPSRFSGSGSGTDFTLTISSLQPSDIATYYCQQWSRNPPTFGQGTK
L3 chain (53) SKLASGVPARFSGSGSGTDYTLTISSLQPEDFATYYCQQWSRNPPTFGGGTK
Consensus (53) SKLASGVPARFSGSGSGTDYTLTISSLQPEDFATYYCQQWSRNPPTFGGGTK
Section 3
(105) 105108
Cris7 VL mouse (105) LQIT
L4 chain (103) VEIK
L1 chain (105) LQIT
L2 chain (105) LQIT
L3 chain (105) VEIK
Consensus (105) LQIT

FIG. 4

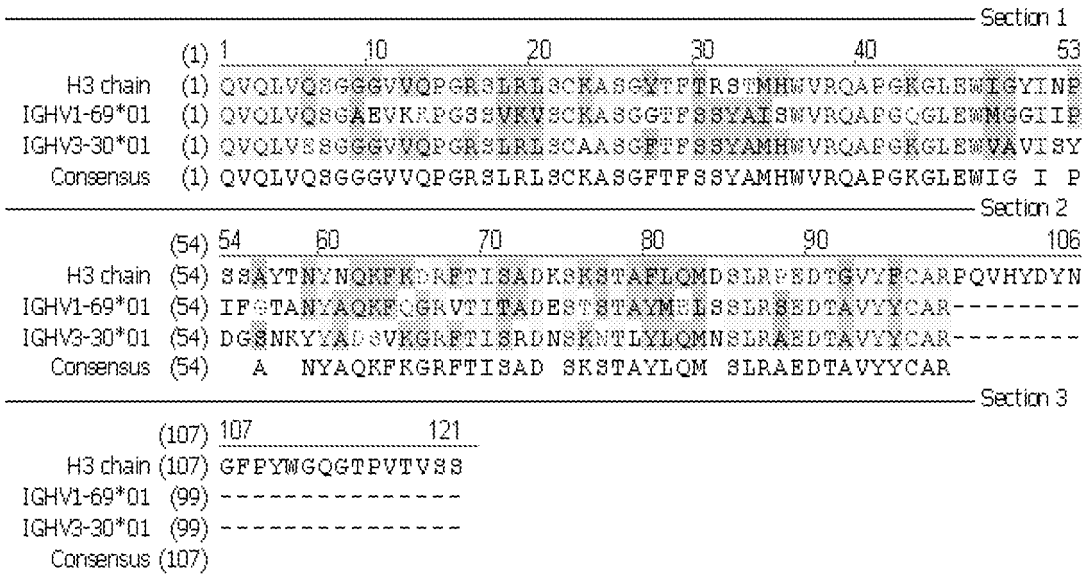

Section 1
(1) 1 10 20 30 40 53
H3 chain (1) QVQLVQSGGGVVQPGRSLRLSCKASGXTFTRSTMHWVRQAPGKGLEWIGYINP
IGHV1-69*01 (1) QVQLVQSGAEVKKPGSSVKVSCKASGGTFSSYAISWVRQAPGQGLEWMGGIIP
IGHV3-30*01 (1) QVQLVESGGGVVQPGRSLRLSCAASGFTFSSYAMHWVRQAPGKGLEWVAVISY
Consensus (1) QVQLVQSGGGVVQPGRSLRLSCKASGFTFSSYAMHWVRQAPGKGLEWIG I P
Section 2
(54) 54 60 70 80 90 106
H3 chain (54) SSAYTNYNQKFKDRFTISADKSKSTAFLQMDSLRVEDTGVYFCARPQVHYDYN
IGHV1-69*01 (54) IFGTANYAQKFQGRVTITADESTSTAYMELSSLRSEDTAVYYCAR--------
IGHV3-30*01 (54) DGSNKYYADSVKGRFTISRDNSKNTLYLQMNSLRAEDTAVYYCAR--------
Consensus (54) A NYAQKFKGRFTISAD SKSTAYLQM SLRAEDTAVYYCAR
Section 3
(107) 107 121
H3 chain (107) GFPYWGQGTPVTVSS
IGHV1-69*01 (99) ---------------
IGHV3-30*01 (99) ---------------
Consensus (107)

FIG. 5

Jk region
IGKV1-5*01
L1 chain
Consensus
Section 1
Section 2
Section 3
JK4 is a better fit
because of sequence
Similarity to the end
of the CDR3 sequence
Species
Gene
Allele
AccNum
Domain label
Functionality
Sequence
Homsap IGKJ1 IGKJ1*01 J00242 F WTFGQGTKVEIK
Homsap IGKJ2 IGKJ2*01 J00242 F YTFGQGTKLEIK
Homsap IGKJ3 IGKJ3*01 J00242 F FTFGPGTKVDIK
Homsap IGKJ4 IGKJ4*01 J00242 F LTFGGGTKVEIK
Homsap IGKJ5 IGKJ5*01 J00242 F ITFGQGTRLEIK

FIG. 6

Section 1
Section 2
Section 3
Translation of DRA209
Translation of DRA219
Translation of DRA222
Translation of DRA221
Translation of DRA223
Translation of DRA224
Translation of DRA225
Consensus

FIG. 7A

Section 4
Section 5
Section 6
Translation of DRA209
Translation of DRA219
Translation of DRA222
Translation of DRA221
Translation of DRA223
Translation of DRA224
Translation of DRA225
Consensus

FIG. 7B

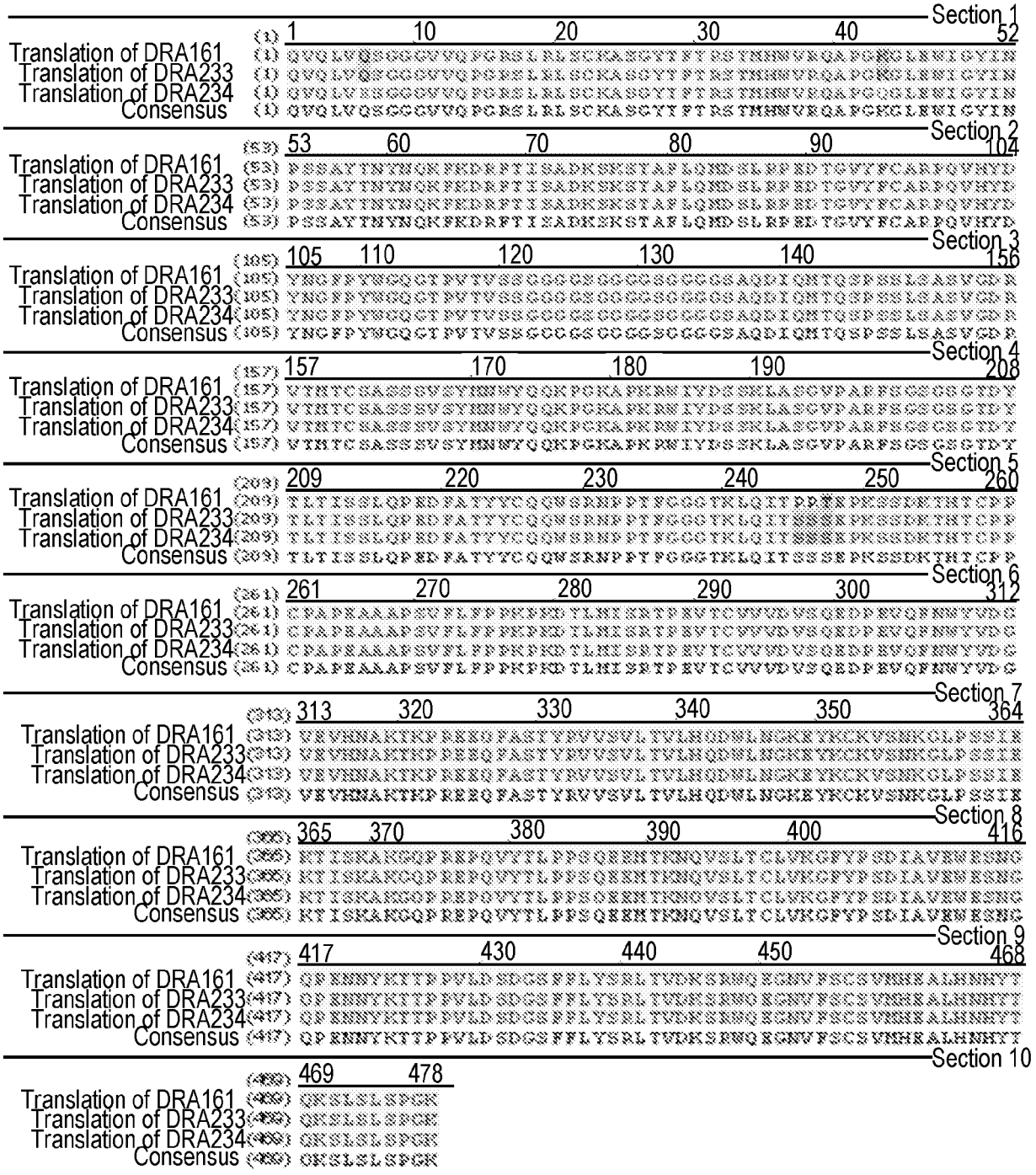

Section 1
Translation of DRA161
Translation of DRA233
Translation of DRA234
Consensus
Section 2
Section 3
Section 4
Section 5
Section 6
Section 7
Section 8
Section 9
Section 10

FIG. 8

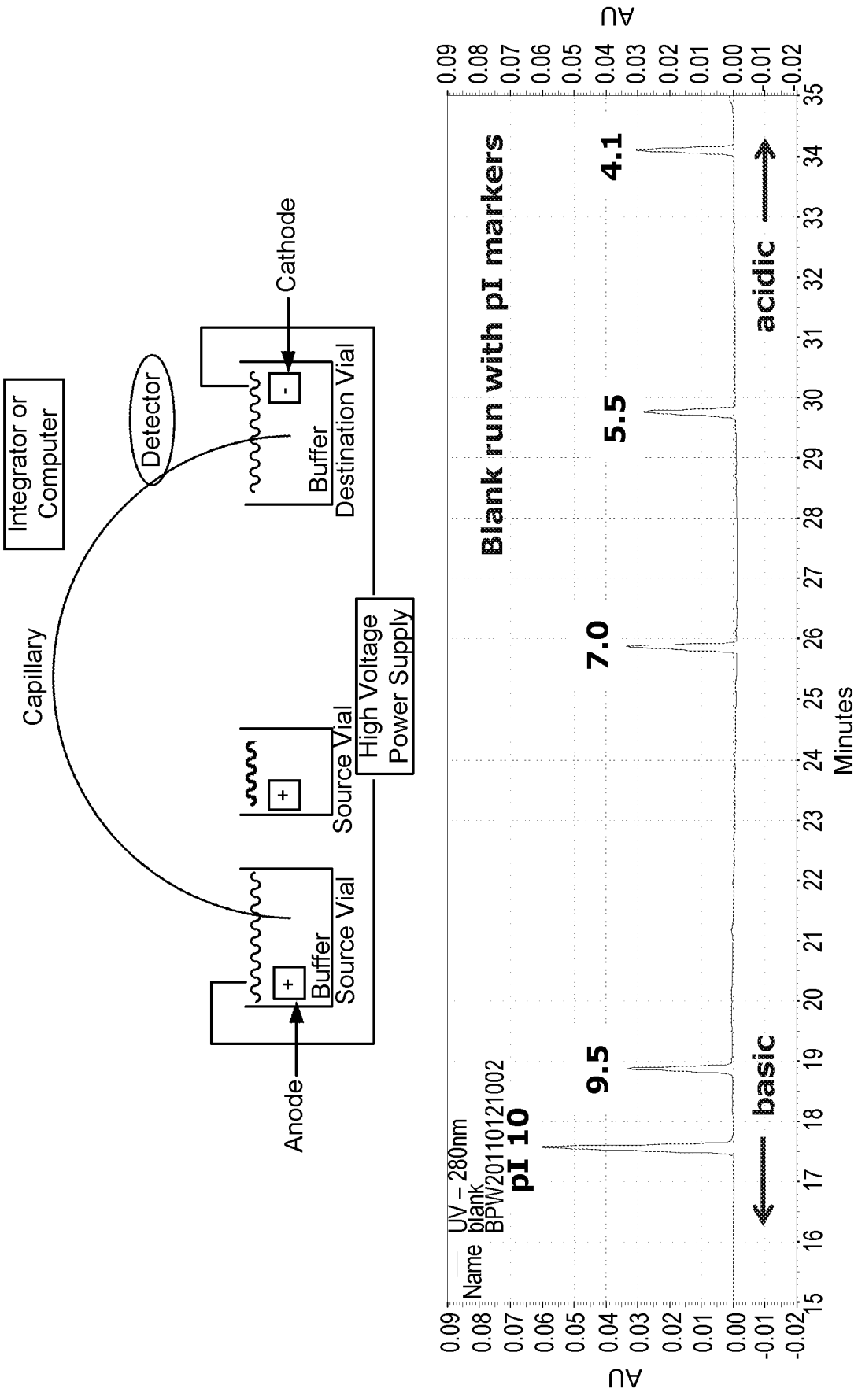

Integrator or Computer
Detector
Capillary
Cathode
Buffer
Destination Vial
Source Vial
High Voltage Power Supply
Anode
Buffer
Source Vial
Blank run with pI markers
pI 10
9.5
7.0
5.5
4.1
basic
acidic
Name UV – 280nm blank BPW20110121002
AU
Minutes

FIG.9

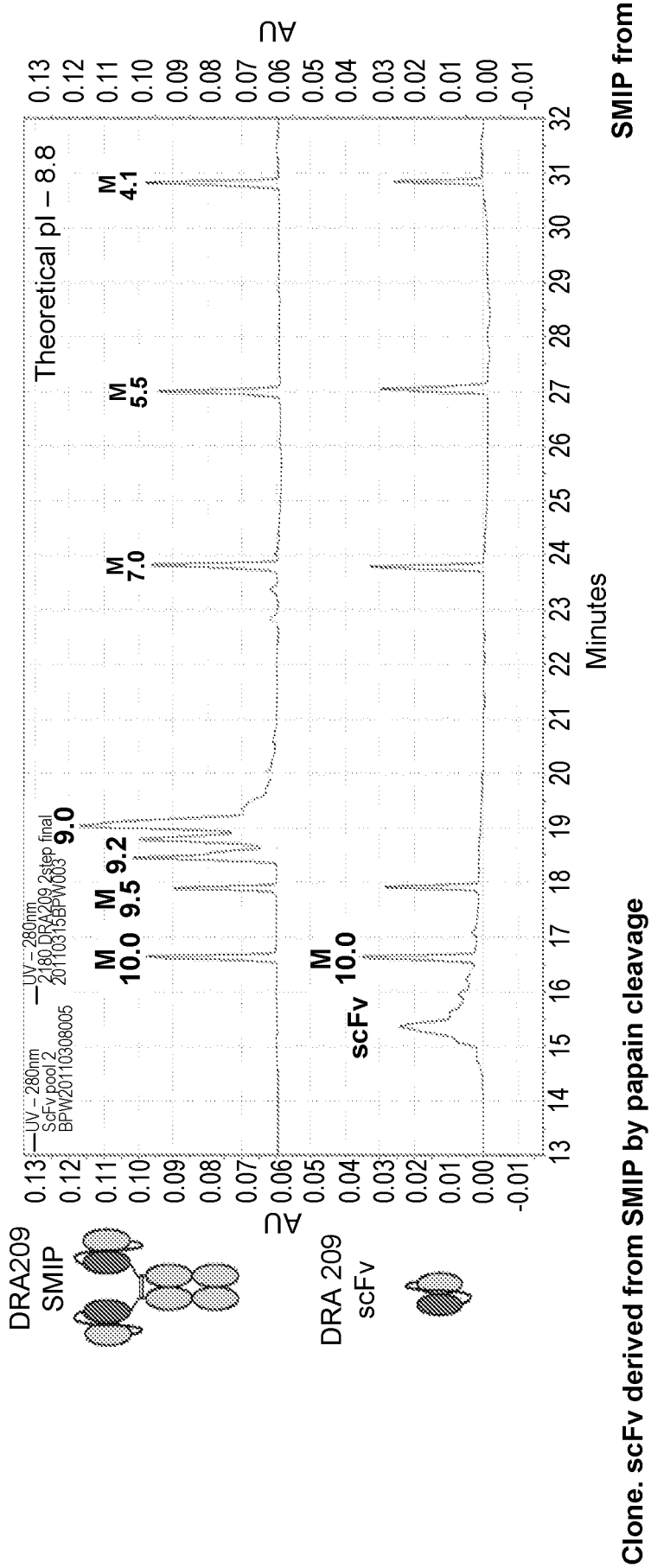

cIEF: Empirical pI of SMIP and scFv Are Even Higher Than Theoretical pI
DRA209 SMIP
DRA 209 scFv
UV – 280nm ScFv pool 2 BPW20110308005
UV – 280nm 2180 DRA209 2step final 20110315BPW003
Theoretical pI – 8.8
M 10.0
M 9.5
M 9.2
9.0
M 7.0
M 5.5
M 4.1
M 10.0
scFv
AU
Minutes
SMIP from CHO
Clone. scFv derived from SMIP by papain cleavage

FIG. 10

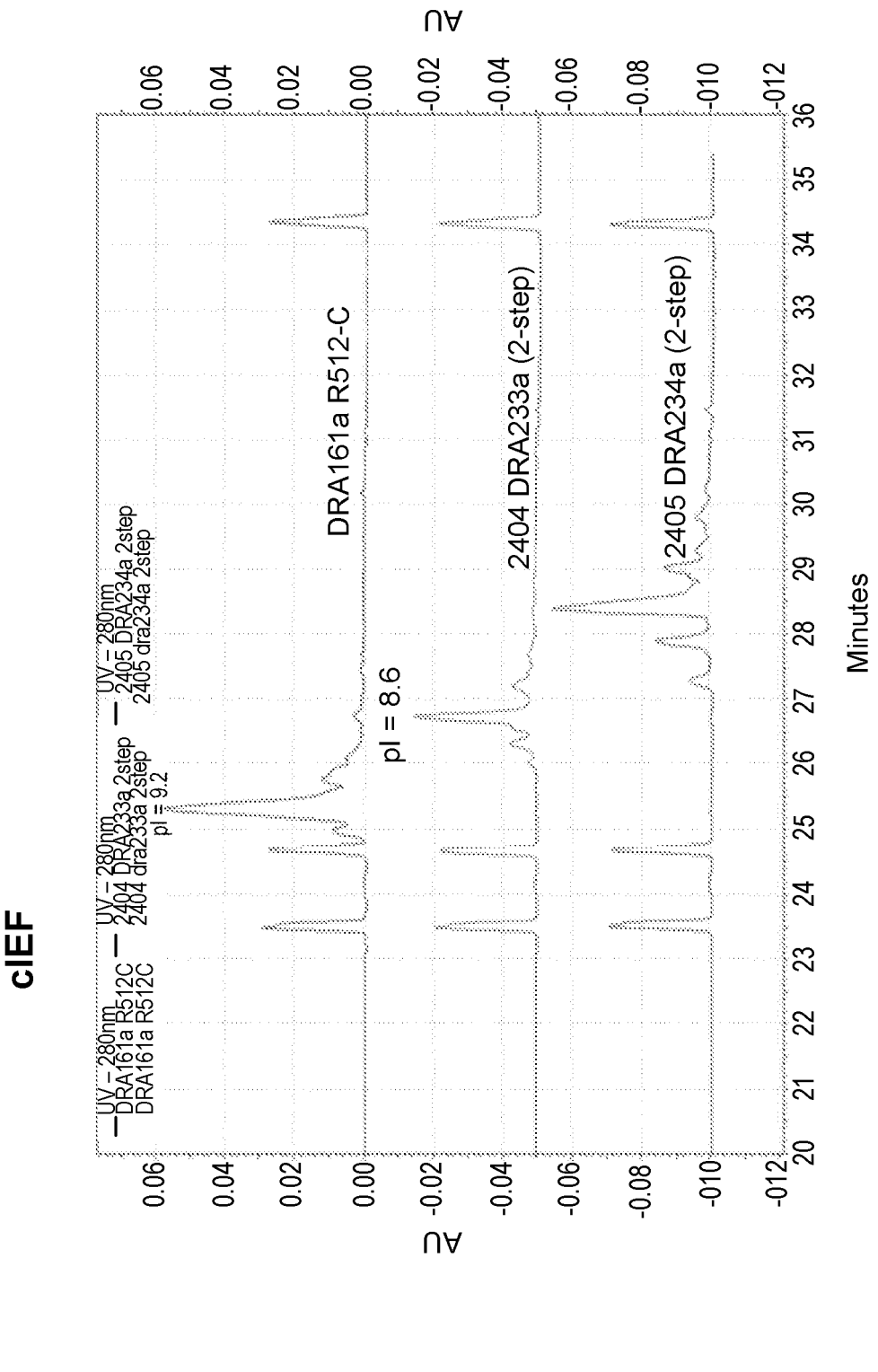

cIEF
UV – 280nm
DRA161a R512C
DRA161a R512C
UV – 280nm
2404 DRA233a 2step
2404 dra233a 2step
pI = 9.2
UV – 280nm
2405 DRA234a 2step
2405 dra234a 2step
DRA161a R512-C
pI = 8.6
2404 DRA233a (2-step)
2405 DRA234a (2-step)
AU
Minutes
DRA233a and DRA234a Expressed in CHO cells

FIG. 11

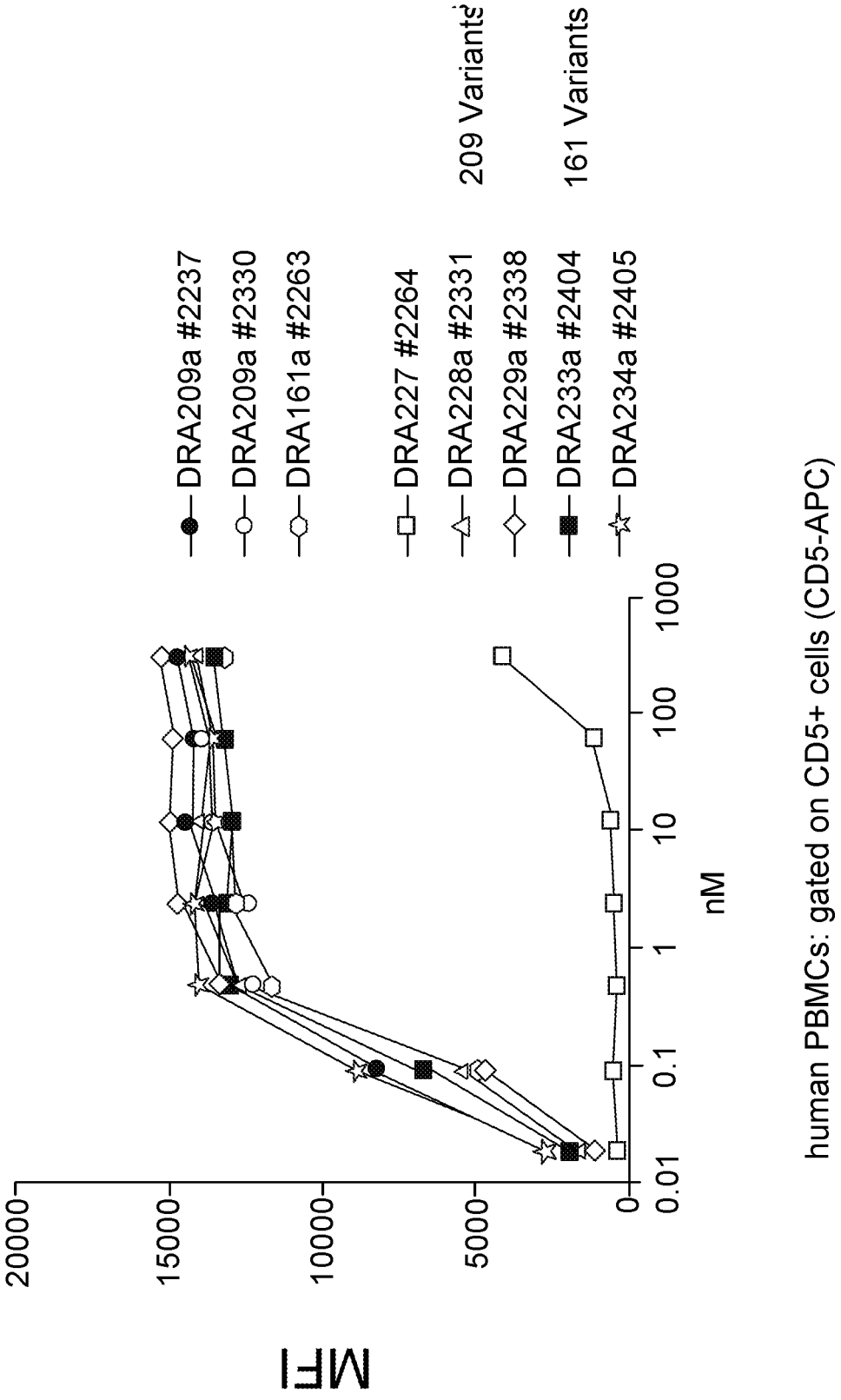
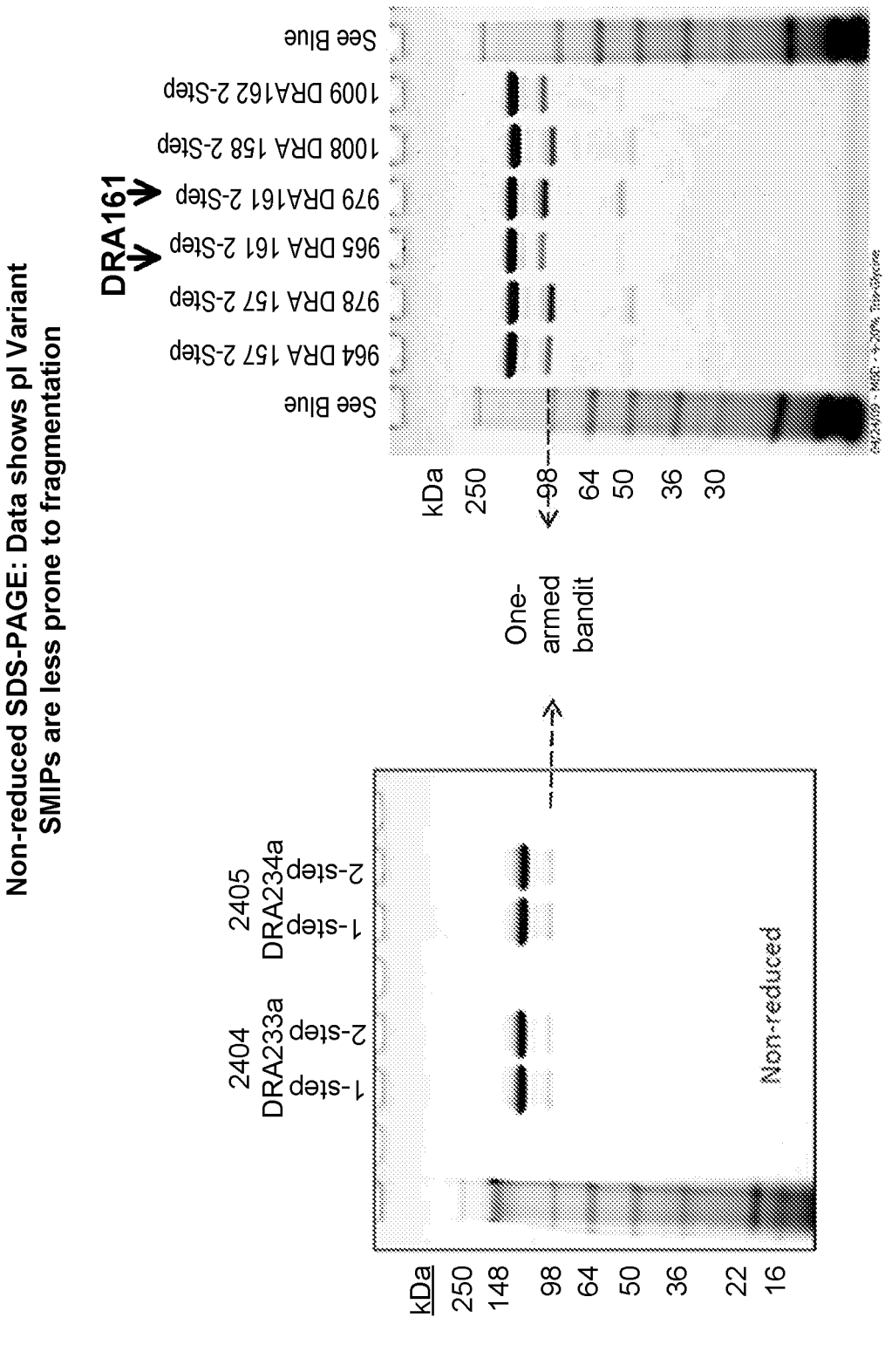

MFI
20000
15000
10000
5000
0
0.01
0.1
1
10
100
1000
nM
human PBMCs: gated on CD5+ cells (CD5-APC)
DRA209a #2237
DRA209a #2330
DRA161a #2263
209 Variants
DRA227 #2264
DRA228a #2331
DRA229a #2338
DRA233a #2404
DRA234a #2405
161 Variants

FIG. 12



DRA161a, DRA233a and DRA234a Expressed in CHO cells (Bulk)

FIG. 13

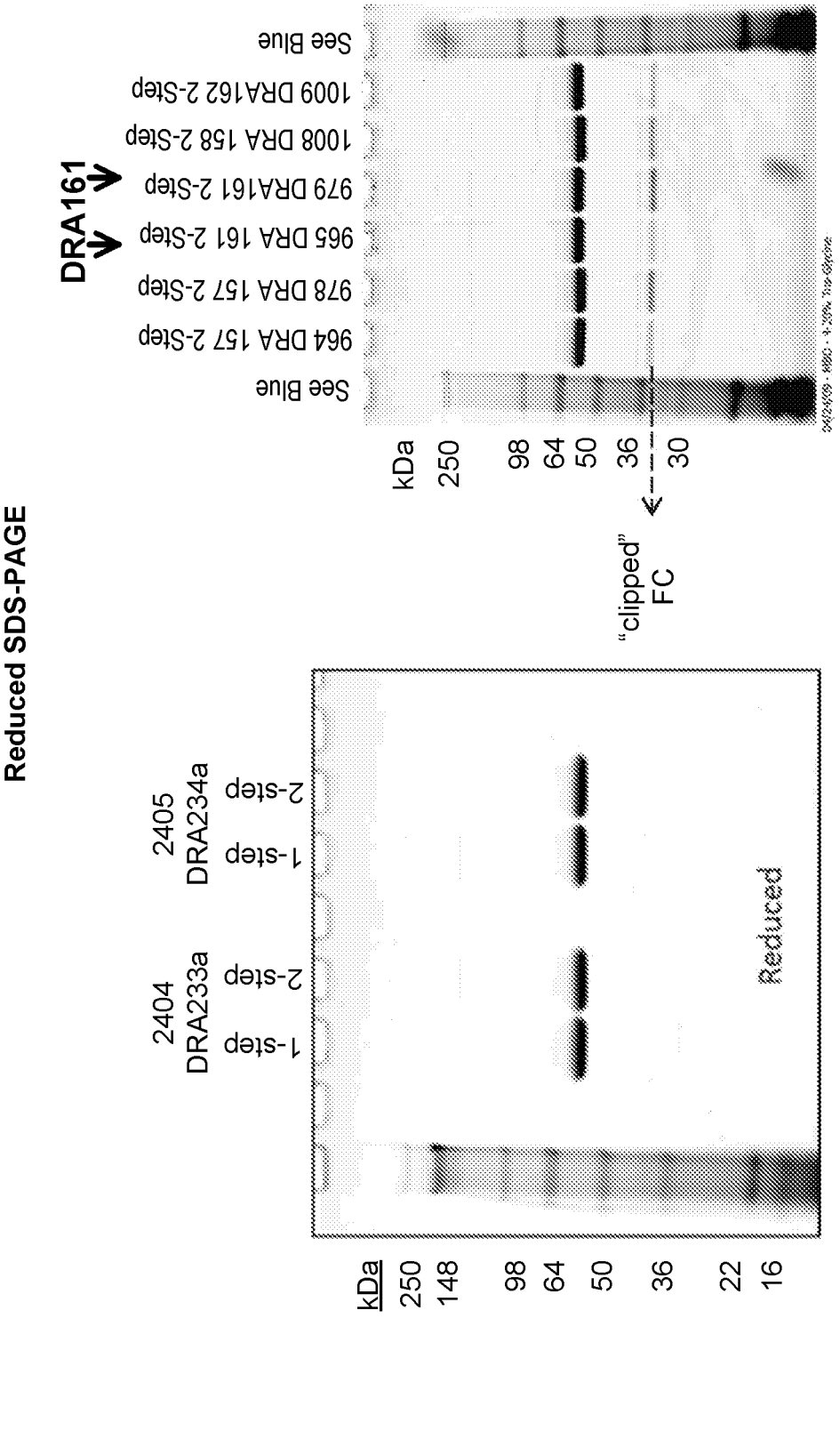
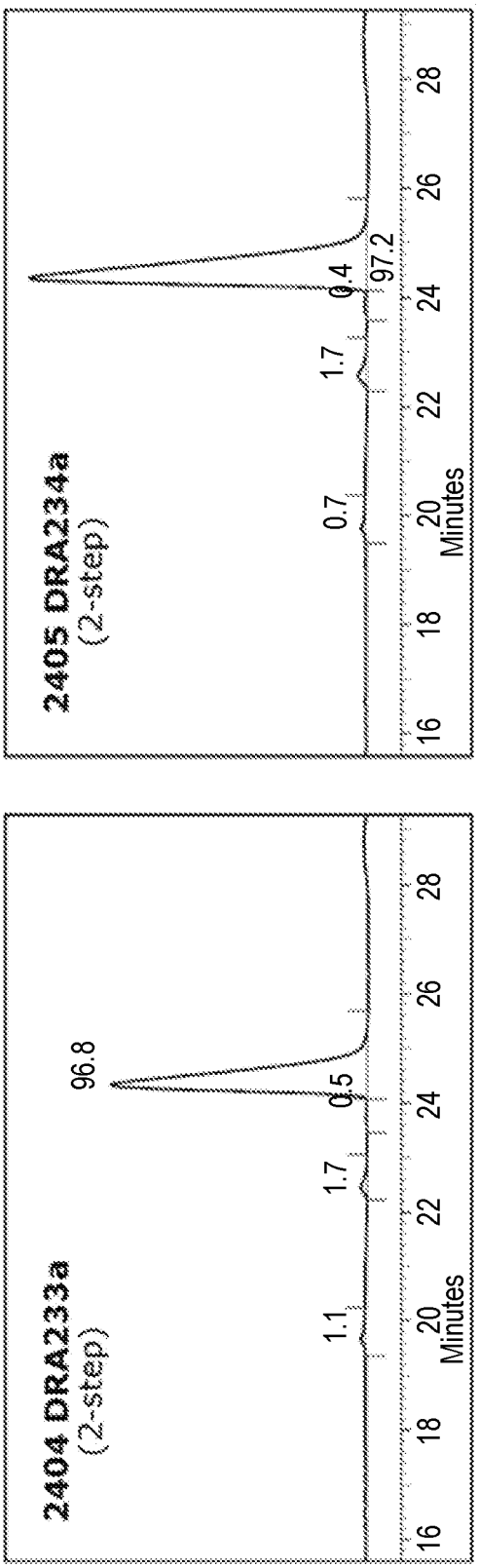

Reduced SDS-PAGE
DRA161a, DRA233a and DRA234a Expressed in CHO cells (Bulk)
kDa
250
148
98
64
50
36
22
16
2404 DRA233a
1-step
2-step
2405 DRA234a
1-step
2-step
Reduced
"clipped" FC
DRA161
See Blue
964 DRA 157 2-Step
978 DRA 157 2-Step
965 DRA 161 2-Step
979 DRA161 2-Step
1008 DRA 158 2-Step
1009 DRA162 2-Step
See Blue

FIG. 14

Non-reduced CE-SDS of pI Variant SMIPs



Sample	% Area by CE-SDS	
	"One-armed bandit"	Intact
2404 DRA233a	1.7	96.8
2405 DRA234a	1.7	97.2

FIG. 15

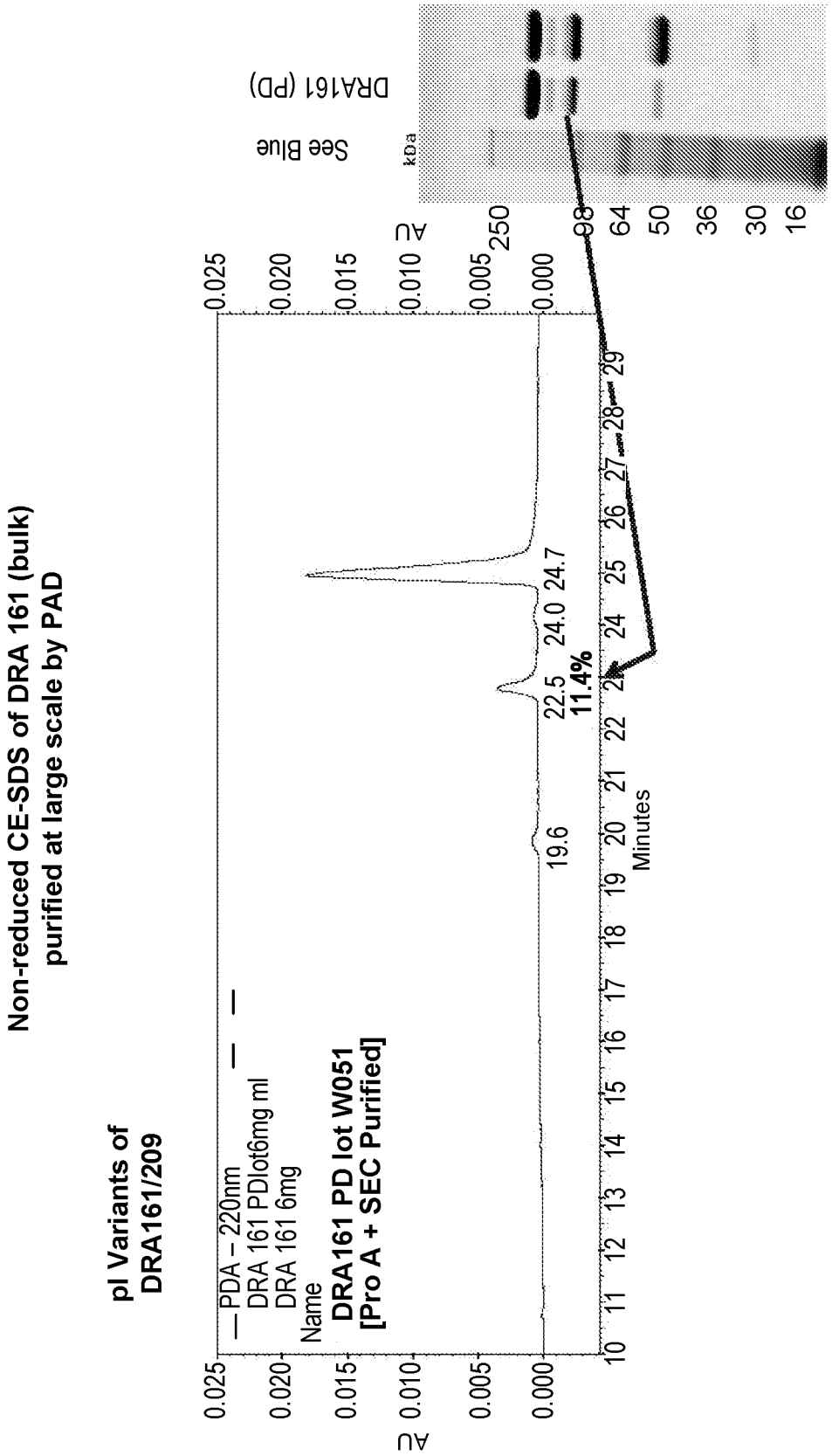

Non-reduced CE-SDS of DRA 161 (bulk)
purified at large scale by PAD
pI Variants of
DRA161/209
PDA – 220nm
DRA 161 PDlot6mg ml
DRA 161 6mg
Name
DRA161 PD lot W051
[Pro A + SEC Purified]
AU
Minutes
19.6
22.5
24.0
24.7
11.4%
See Blue
DRA161 (PD)
kDa
250
98
64
50
36
30
16

FIG. 16

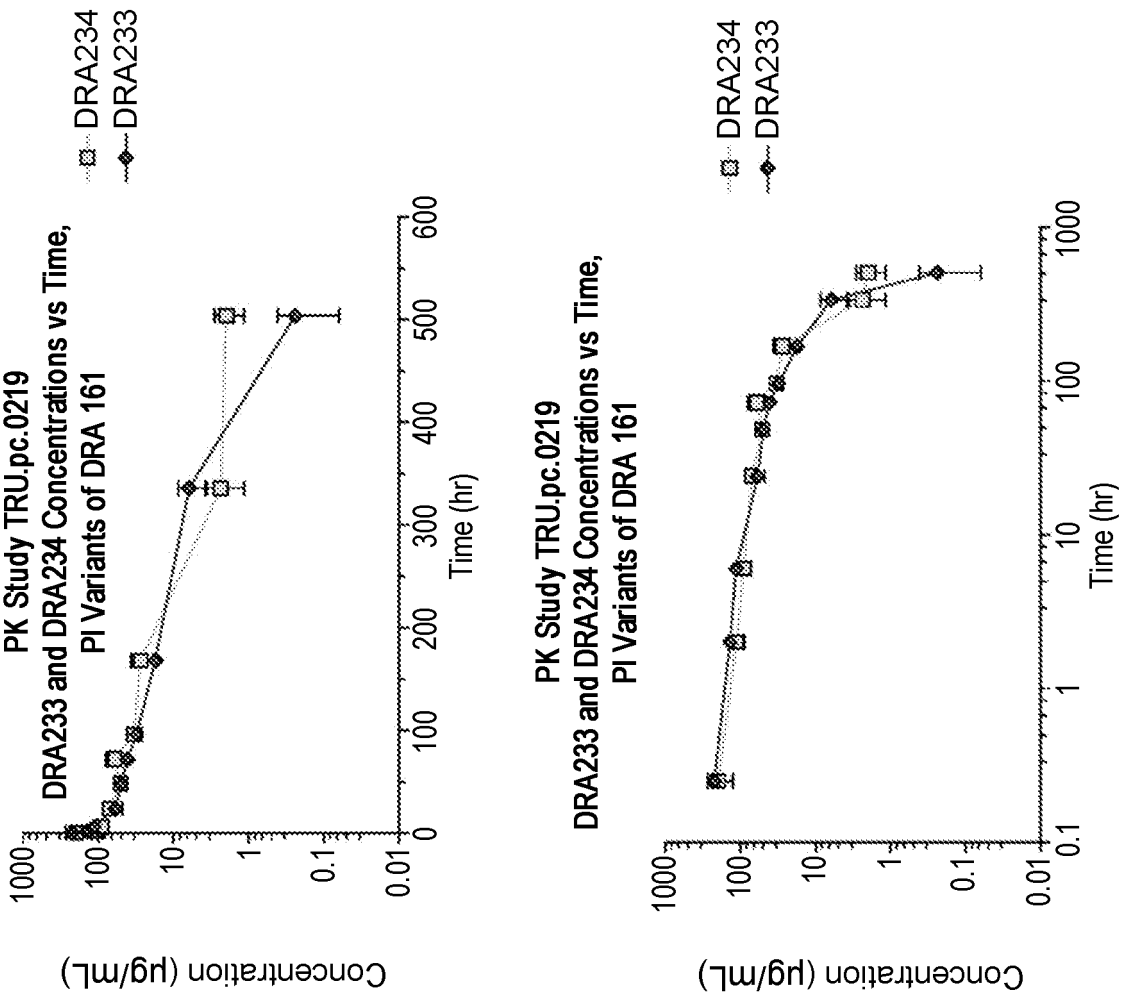

PK Study TRU.pc.0219
DRA233 and DRA234 Concentrations vs Time,
PI Variants of DRA 161
DRA234
DRA233
Concentration (µg/mL)
Time (hr)
1000
100
10
1
0.1
0.01
0
100
200
300
400
500
600
PI Variants of DRA161/209
Concentration over time for DRA233 and DRA234

FIG. 17

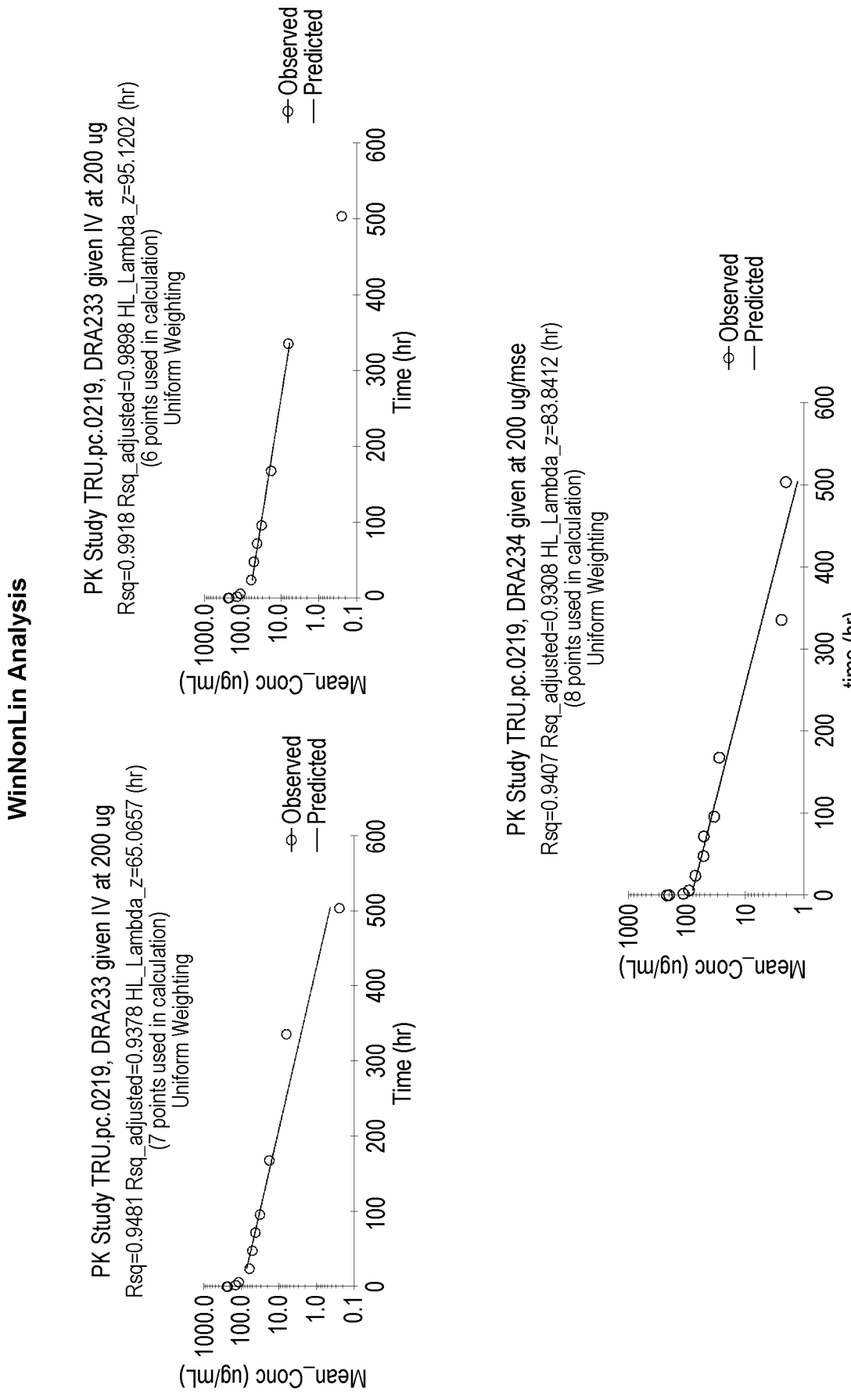

WinNonLin Analysis
PK Study TRU.pc.0219, DRA233 given IV at 200 ug
Rsq=0.9481 Rsq_adjusted=0.9378 HL_Lambda_z=65.0657 (hr)
(7 points used in calculation)
Uniform Weighting
Mean_Conc (ug/mL)
Time (hr)
Observed
Predicted
PK Study TRU.pc.0219, DRA233 given IV at 200 ug
Rsq=0.9918 Rsq_adjusted=0.9898 HL_Lambda_z=95.1202 (hr)
(6 points used in calculation)
Uniform Weighting
Mean_Conc (ug/mL)
Time (hr)
Observed
Predicted
PK Study TRU.pc.0219, DRA234 given at 200 ug/mse
Rsq=0.9407 Rsq_adjusted=0.9308 HL_Lambda_z=83.8412 (hr)
(8 points used in calculation)
Uniform Weighting
Mean_Conc (ug/mL)
time (hr)
Observed
Predicted

FIG. 18

	Estimate	Units	DRA233 w/o 504 hr	DRA233	DRA234
pI Variants of DRA 161/209	Rsq		0.9918	0.9481	0.9407
	Rsq_adjusted		0.9898	0.9378	0.9308
	Corr_XY		-0.9959	-0.9737	-0.9699
	No_points_lambda_z		6	7	8
	Lambda_z	1/hr	0.0073	0.0107	0.0083
	Lambda_z_lower	hr	24	24	6
	Lambda_z_upper	hr	336	504	504
	HL_Lambda_z	**hr**	**95.12**	**65.07**	**83.84**
PK Estimates for DRA233 and DRA234	Tmax	hr	0.25	0.25	0.25
	Cmax	ug/mL	223.67	223.67	198.91
	SE_Cmax	ug/mL	14.44	14.44	42.40
	Cmax_D	kg*ug/mL/mg	20.98	20.98	18.84
	C0	ug/mL	239.3	239.3	215.5
	Tlast	hr	504	504	504
	Clast	ug/mL	0.2412	0.2412	2.0063
	AUClast	hr*ug/mL	10029	10029	10991
	SE_AUClast	hr*ug/mL	363.4	363.4	278.1
	AUCall	hr*ug/mL	10029	10029	10991
	SE_AUCall	hr*ug/mL	363.4	363.4	278.1
	AUCINF_obs	hr*ug/mL	10062	10051	11234
	AUCINF_D_obs	hr*kg*ug/mL/mg	943.9	942.9	1063.8
	AUC_%Extrap_obs	%	0.329	0.225	2.160
	AUC_%Back_Ext_obs	%	0.575	0.576	0.4612
	Vz_obs	**mL/kg**	**145.39**	**99.55**	**113.7**
	Cl_obs	**mL/hr/kg**	**1.059**	**1.061**	**0.94**
	AUMClast	hr*hr*ug/mL	1027660	1027660	1122005
	AUMCINF_obs	hr*hr*ug/mL	1048881	1041195	1273670
	AUMC_%Extrap_obs	%	2.023	1.300	11.91
	MRTlast	hr	102.47	102.47	102.08
	MRTINF_obs	hr	104.24	103.59	113.38
	Vss_obs	mL/kg	110.44	109.86	106.58
	mean dose	mg/kg	10.66	10.66	10.56

FIG. 19

pI Variants of DRA161/209

Humanized CRIS7 Constructs: Comparison of PK parameters

Parameter	Estimates			
	DRA161	DRA233 w/o 504 hr*	DRA233	DRA234
Empirical pI	9.2	8.6	8.6	8.0
(Half-life, hr)	59.3	95.1	65.1	83.8
(Clearance, mL/hr/kg)	2.15	1.1	1.1	0.9

* Excluding the last time point

DRA 234 shows significantly higher half-life than DRA 161

FIG. 20

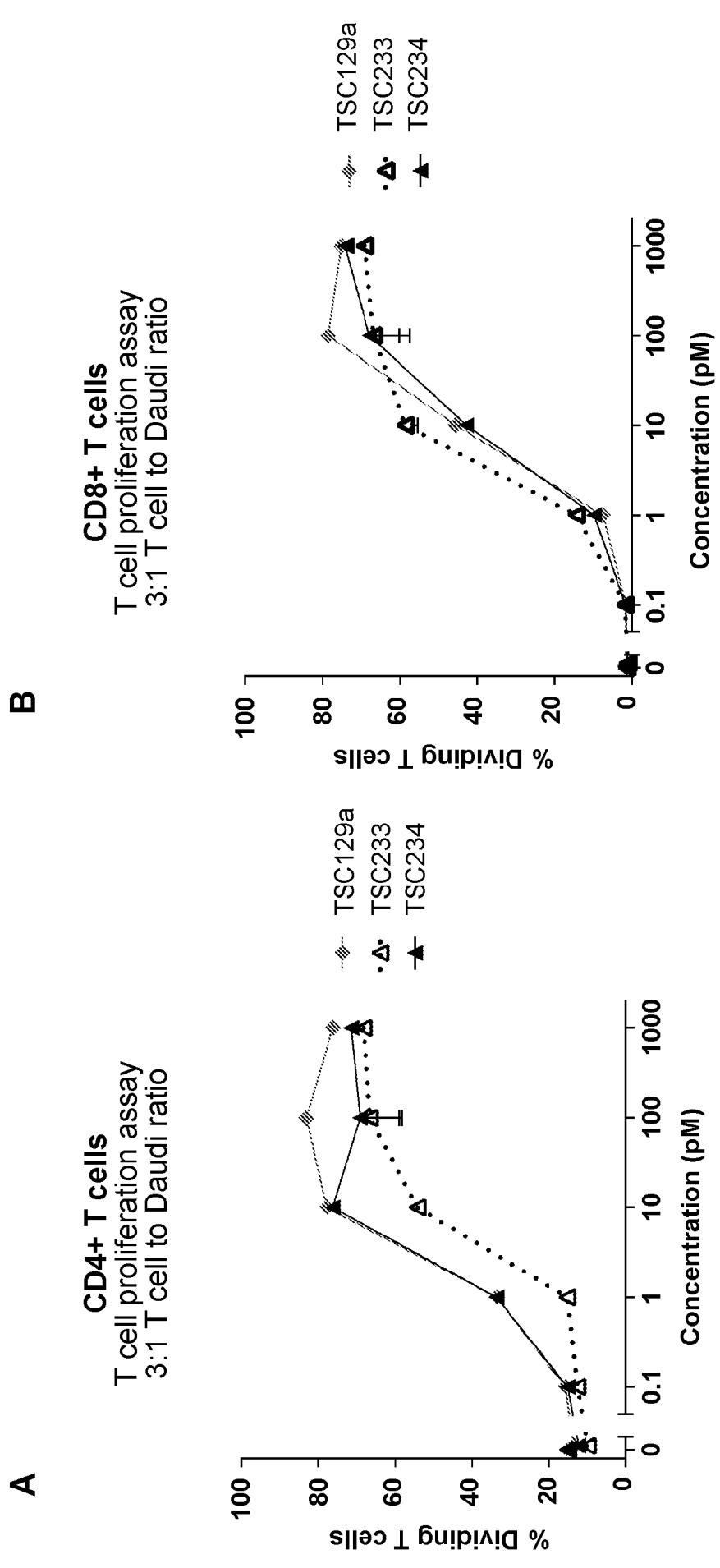

A
CD4+ T cells
T cell proliferation assay
3:1 T cell to Daudi ratio
% Dividing T cells
Concentration (pM)
TSC129a
TSC233
TSC234
B
CD8+ T cells
T cell proliferation assay
3:1 T cell to Daudi ratio
% Dividing T cells
Concentration (pM)
TSC129a
TSC233
TSC234

FIG. 21

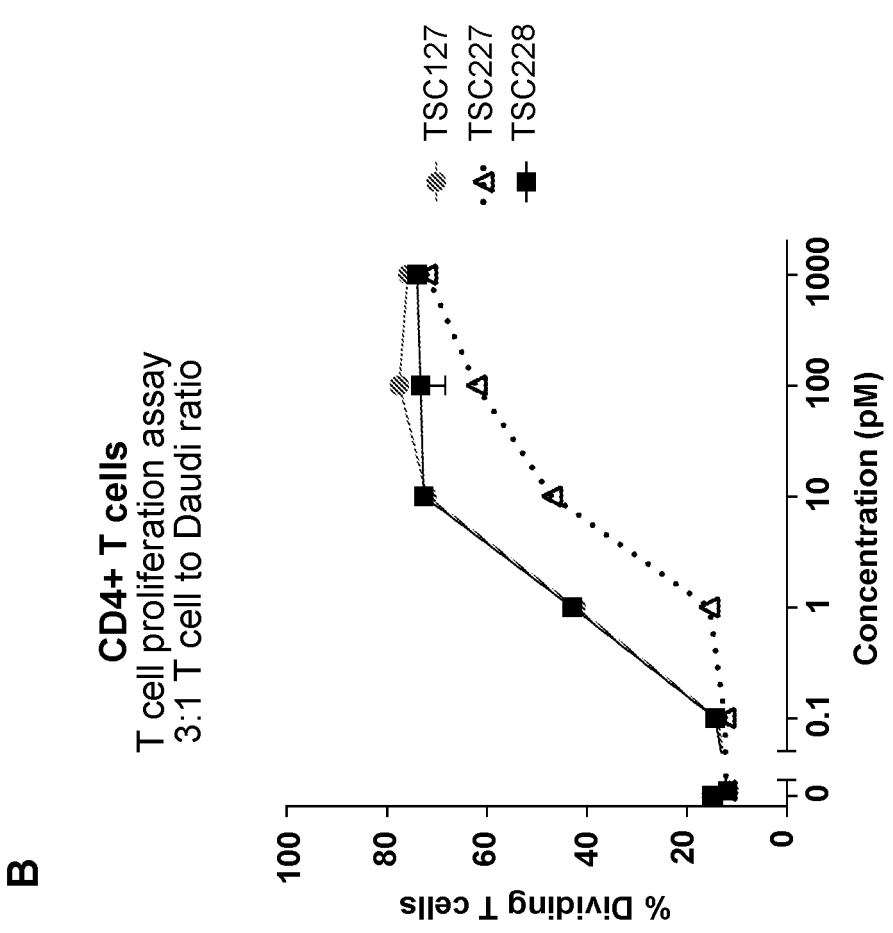

A
CD8+ T cells
T cell proliferation assay
3:1 T cell to Daudi ratio
% Dividing T cells
Concentration (pM)
TSC127
TSC227
TSC228
B
CD4+ T cells
T cell proliferation assay
3:1 T cell to Daudi ratio
% Dividing T cells
Concentration (pM)
TSC127
TSC227
TSC228

FIG. 22

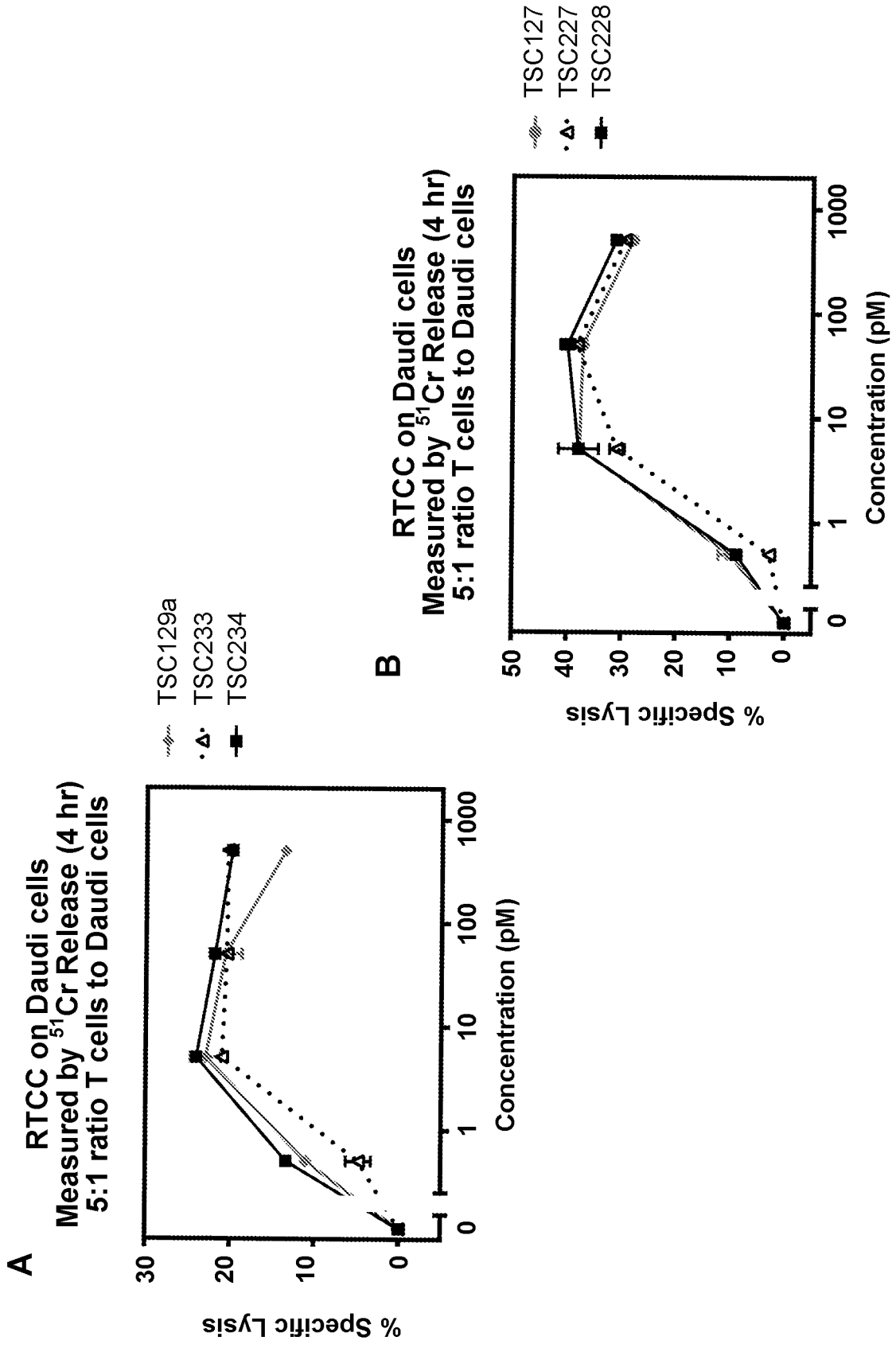

A
RTCC on Daudi cells
Measured by 51Cr Release (4 hr)
5:1 ratio T cells to Daudi cells
% Specific Lysis
Concentration (pM)
TSC129a
TSC233
TSC234
B
RTCC on Daudi cells
Measured by 51Cr Release (4 hr)
5:1 ratio T cells to Daudi cells
% Specific Lysis
Concentration (pM)
TSC127
TSC227
TSC228

FIG. 23

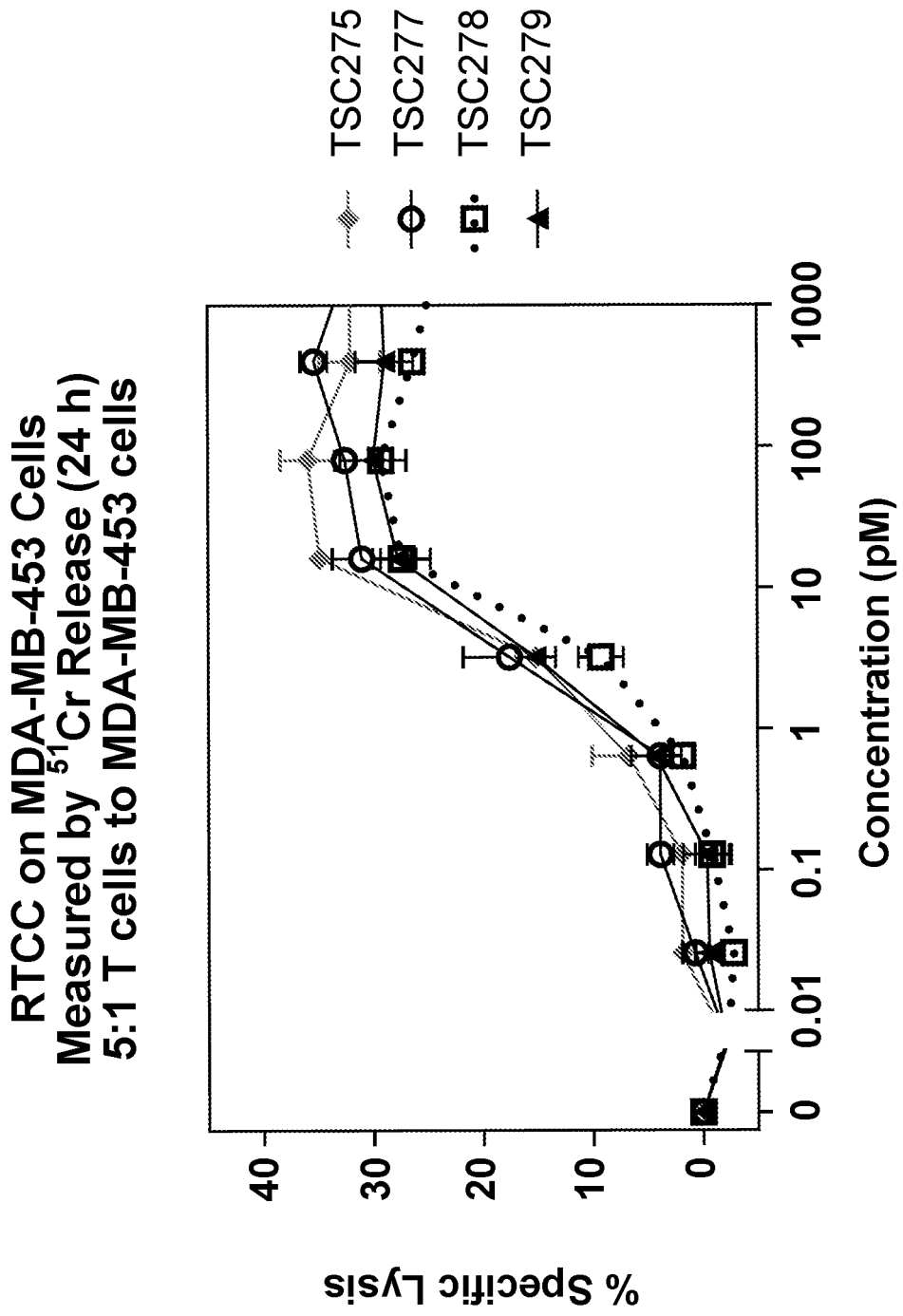

RTCC on MDA-MB-453 Cells
Measured by 51Cr Release (24 h)
5:1 T cells to MDA-MB-453 cells
TSC275
TSC277
TSC278
TSC279
% Specific Lysis
0
10
20
30
40
0
0.01
0.1
1
10
100
1000
Concentration (pM)

FIG. 24

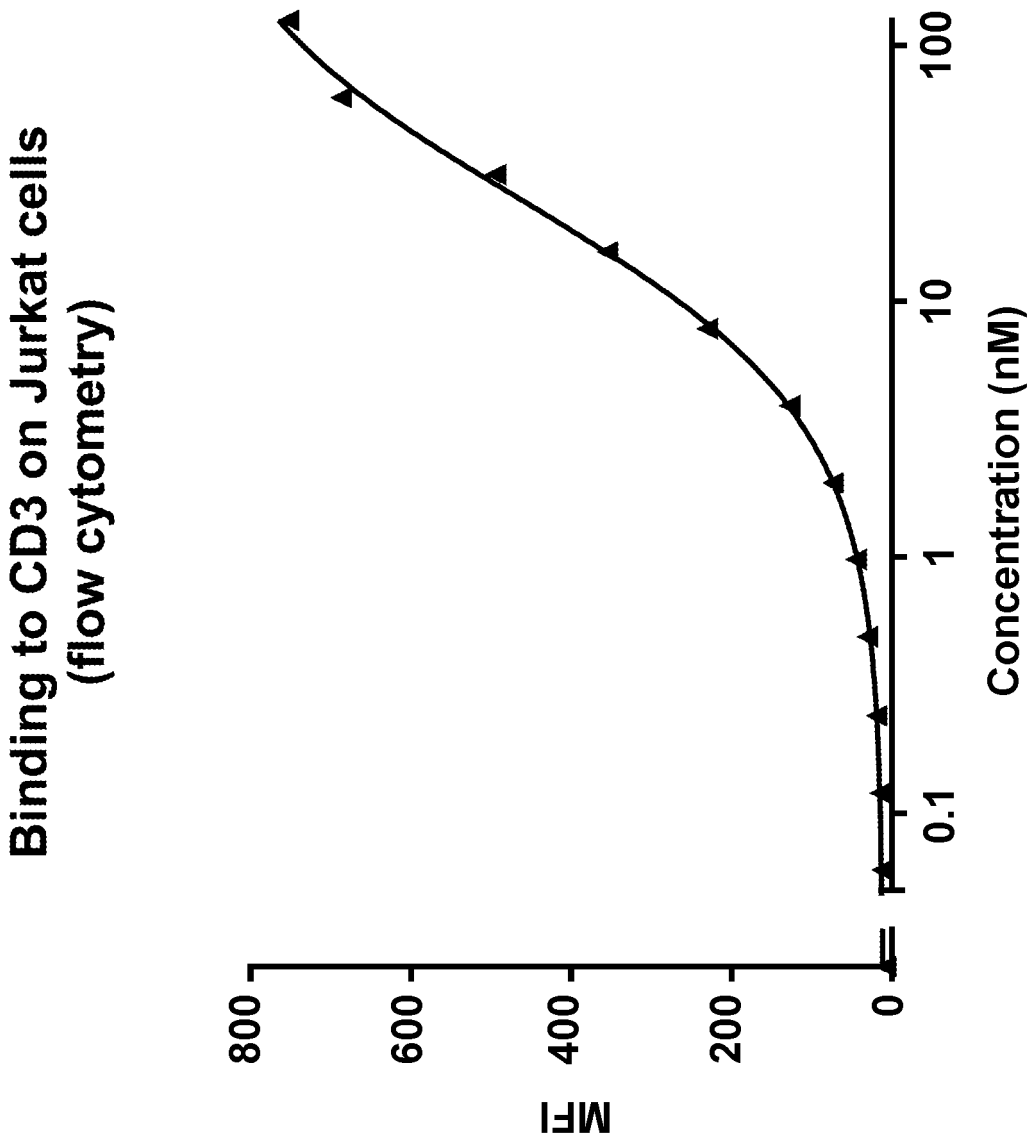

Binding to CD3 on Jurkat cells
(flow cytometry)
MFI
800
600
400
200
0
0.1
1
10
100
Concentration (nM)
TSC228

FIG. 25A

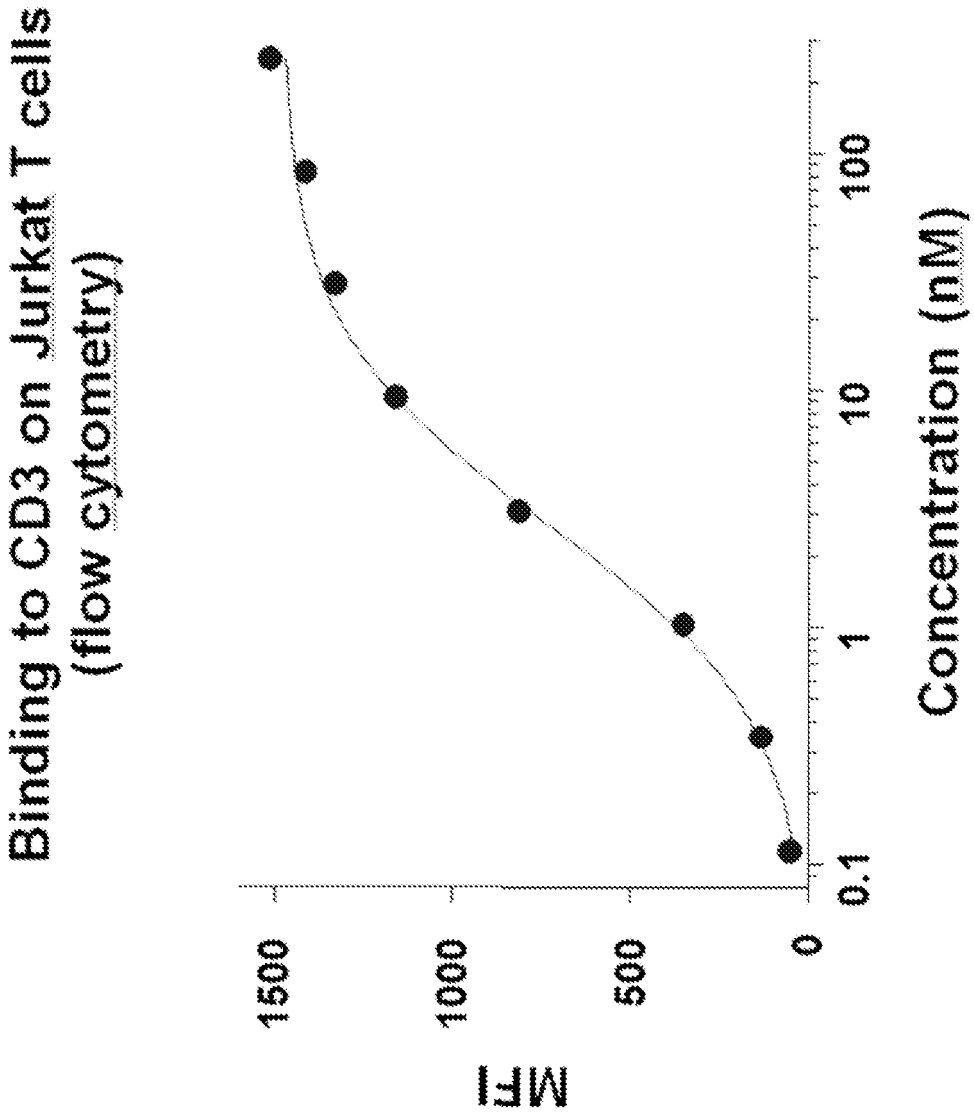

Binding to CD3 on Jurkat T cells
(flow cytometry)
MFI
1500
1000
500
0
0.1
1
10
100
Concentration (nM)
TSC249

FIG. 25B

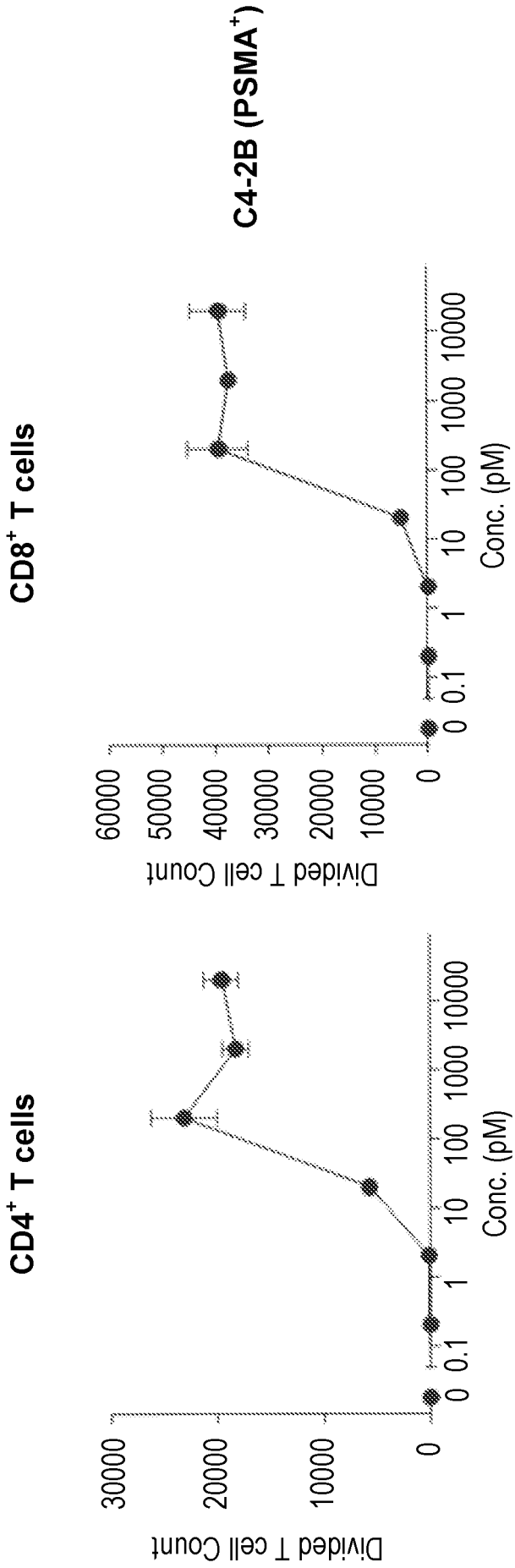

C4-2B (PSMA+)
CD8+ T cells
CD4+ T cells
Divided T cell Count
Conc. (pM)
0
10000
20000
30000
40000
50000
60000
0
0.1
1
10
100
1000
10000

FIG. 26A

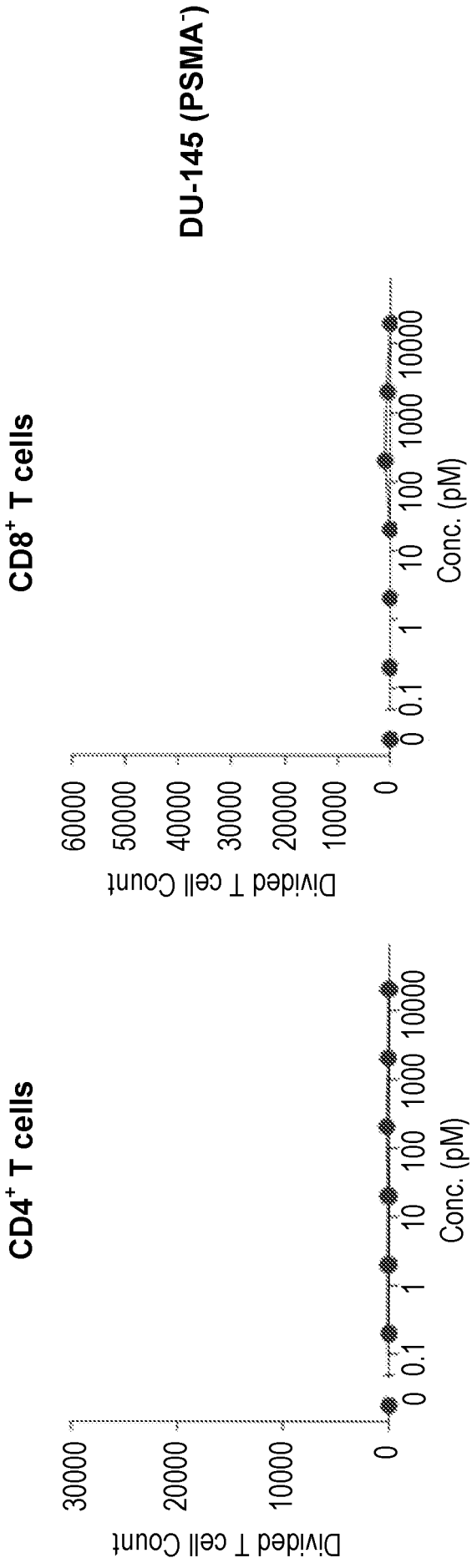

DU-145 (PSMA+)
CD8+ T cells
CD4+ T cells
Divided T cell Count
Conc. (pM)
0
10000
20000
30000
40000
50000
60000
0
0.1
1
10
100
1000
10000

FIG. 26B

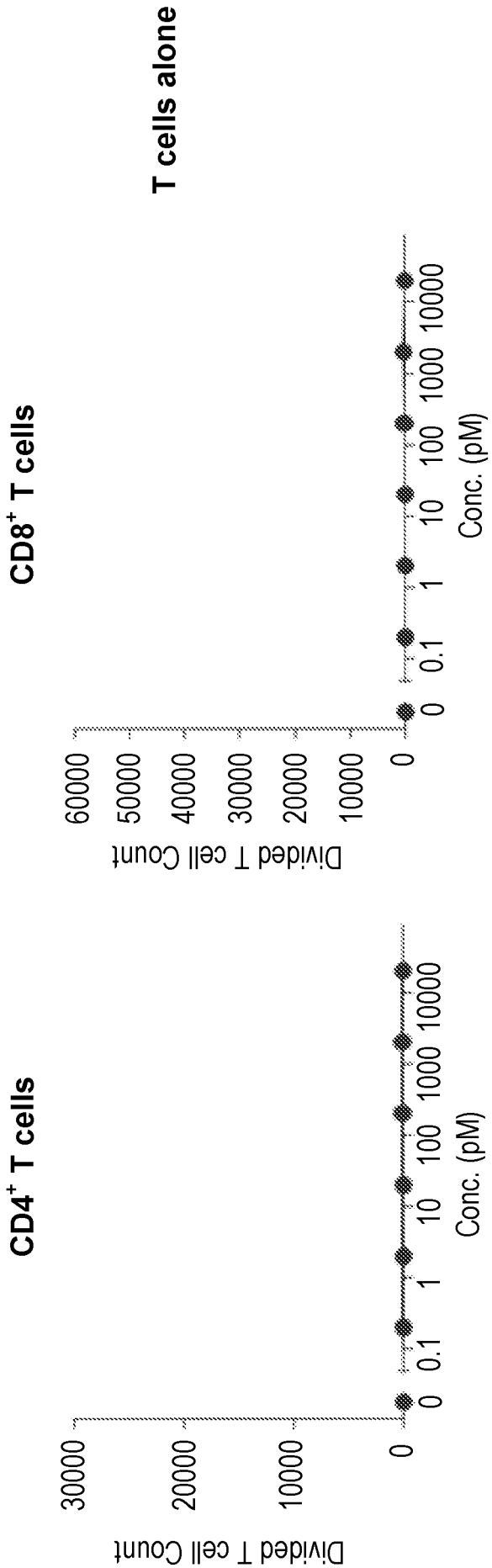

T cells alone
CD8+ T cells
Divided T cell Count
60000
50000
40000
30000
20000
10000
0
0
0.1
1
10
100
1000
10000
Conc. (pM)
CD4+ T cells
Divided T cell Count
30000
20000
10000
0
0
0.1
1
10
100
1000
10000
Conc. (pM)

FIG. 26C

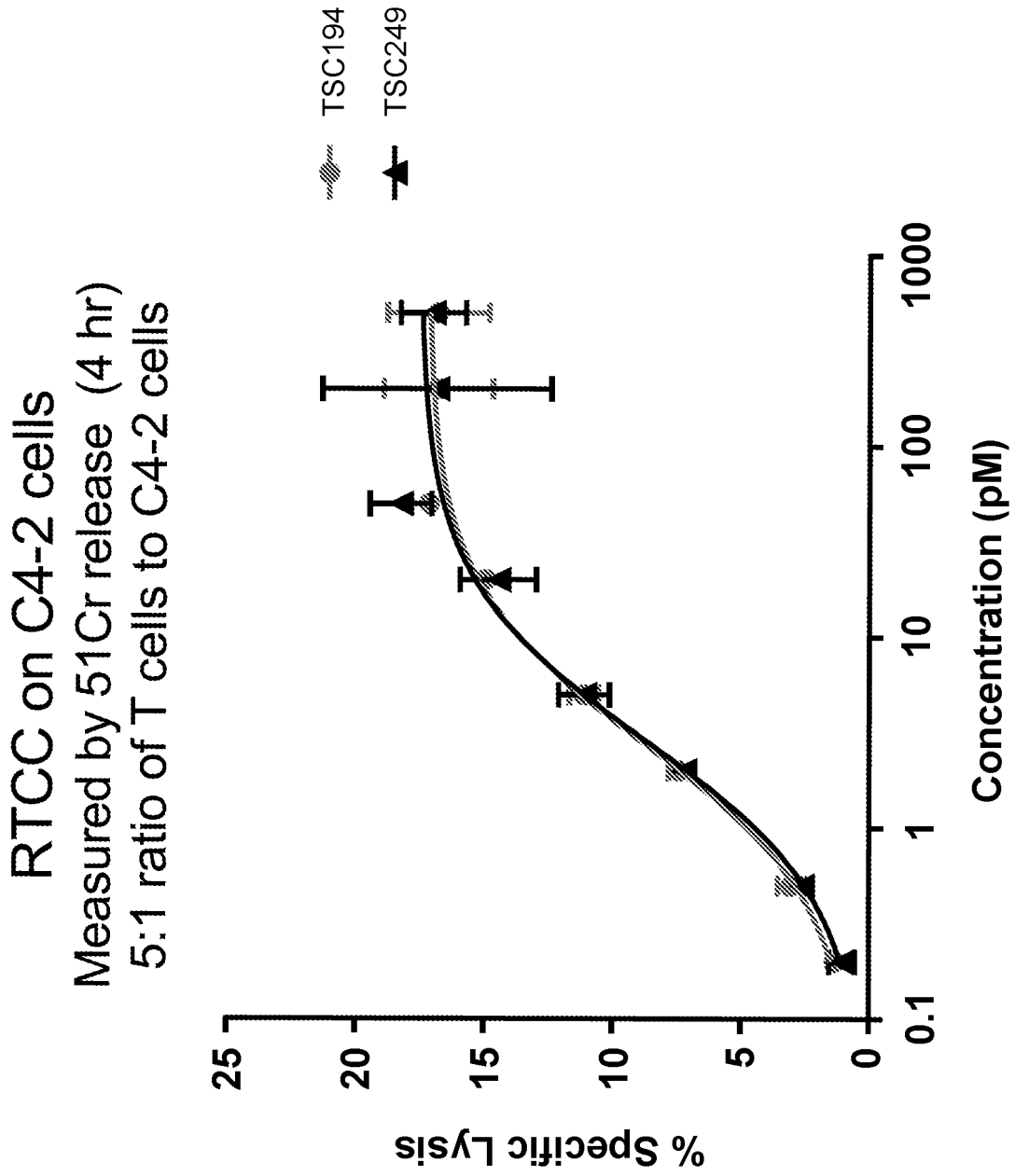

RTCC on C4-2 cells
Measured by 51Cr release (4 hr)
5:1 ratio of T cells to C4-2 cells
TSC194
TSC249
% Specific Lysis
0
5
10
15
20
25
0.1
1
10
100
1000
Concentration (pM)

FIG. 27